Determining particle size distribution and refractive index in a two-layer tissue phantom by linearly polarized light

Yong Deng (邓 勇), Qiang Lu (鲁 强), and Qingming Luo (骆清铭)

Key Laboratory of Biomedical Photonics of Ministry of Education, Huazhong University of Science and Technology, Wuhan, 430074

Received July 11, 2005

We report a new method for measuring particle size distribution (PSD) and refractive index of the top layer in a two-layer tissue phantom simulated epithelium tissue by varying the azimuth angle of incident linearly polarized light. The polarization gating technique is used to decouple the single and multiple scattering components in the returned signal. The theoretical model based on Mie theory is presented and a nonlinear inversion method — floating genetic algorithm — is applied to inverting the azimuth dependence of component of polarization light backscattered. The experiment results demonstrate that the size distribution and refractive index of the scatters of the top layer can be determined by measuring and analyzing the differential signal of the parallel and perpendicular components from a two-layer tissue phantom. The method implies to detect precancerous changes in human epithelial tissue.

OCIS codes: 170.3660, 260.5430, 290.1350, 290.4020.

In recent years, the studies on extracting the information of morphological changes in human epithelial tissue *in situ* without perturbing them have become increasingly important. More than 85% of all cancers originate in the epithelia lining the internal surfaces of human body. Pre-cancers are characterized by increased nuclear size, increased nuclear/cytoplasm ratio, hyperchromasia and polymorphism, which currently can only be assessed through invasive, painful biopsy. Therefore, some potentially important diagnostic information will be lost or altered.

Optics method may provide a non-invasive tool to assess nuclear morphometry. The tissues can be studied in its natural state since tissue biopsy is not necessary and fixation and staining are not required. Epithelial-cell nuclei can be modelled as Mie scattering transparent spheroids whose refractive index is higher than that of the surrounding cytoplasm because of their chromatin content. When the cells are illuminated by visible light, the refractive index difference will result in light scattering. Some of optical techniques have been investigated for a non-invasive tissue diagnosis. The cross polarization optical coherence tomography (CP OCT) provided a map of cross-polarization backscattering properties, which made it possible to differentiate neoplastic and scar changes in the esophagus[1]. Sung presented a fiber optic confocal reflectance microscope (FCRM) which can be used to image epithelial tissue with sub-cellular resolution *in vivo*. The confocal images of normal and abnormal appearing cervical tissue were obtained *in vivo*[2]. Recent interest in the use of light-scattering techniques to measure structural properties has focused on measuring the size of cell nuclei and other subcellular organelles within biological tissues. In particular, light scattering spectroscopy has shown that cell nuclei can be regarded as spherical Mie objects and their size can be determined by comparing the wavelength dependence of their backscattering cross section with theoretical models[3−9]. This technique has been demonstrated to be an effective means in detecting irregularities in the structure of epithelial cell nuclei associated with neoplasia. Bartlett *et al.* reported the ability to use polarized light scattering spectroscopy to measure the particle size distribution (PSD) of thin layers of polystyrene microspheres on top of a solid Intralipid phantom. The optical properties of each layer were adjusted to match the absorption and scattering properties of the epidermis and dermis[10,11]. Amelink reported fiber-optic probe's sensitivity to light scattered from the superficial layers of tissue[12]. In this letter, we explore a new method to directly measure the particles mean size, standard deviation, and refractive index of the top layer in a two-layer phantom simulated epithelium tissue by varying the incident light polarization azimuth.

The measurement setup is shown in Fig. 1. A He-Ne laser (Melles Griot, Inc.) (10 mW) emitting a collimated 1.5-mm $1/e^2$-diameter beam of 632.8-nm radiation is used as light source. The beam passes through a half-wave plate (HWP) and a linear polarizer LP1 which is used to select the polarization azimuth of the incident light, and then is refocused with a small solid angle onto the sample using a lens ($f = 19$ mm). In order to avoid specular reflectance, the incident beam is oriented at an angle of 5° to the normal to the sample surface. The sample is illuminated by a circular spot of light of 0.1 mm

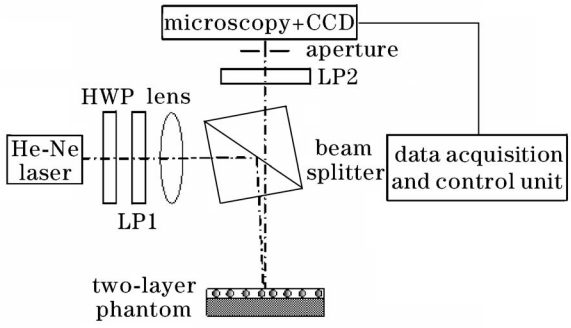

Fig. 1. Schematic diagram of experimental setup for measuring diffusely backscattered polarized light.

in diameter. The diffusely backscattered light emerging from the sample passes through a polarizing beam cube, a polarization analyzer LP2, and an aperture. The output light is collected in a narrow cone and imaged using a microscopy onto a 1392×1040 pixel, 12 bit cooled charge-coupled device (CCD) camera (Princeton Instruments, 512TK).

An analyzer is used to discriminate between light scattered from the top layer and light that has been multiply scattered from the deeper, second layer. The directions of the incident light and scattered light make up the scattering plane. If the incident light is linearly polarized, it is convenient to choose the laboratory system such that the z-axis is along the backscattering direction, the x-axis parallel to the scattering plane, and the y-axis perpendicular to the scattering plane. Thus, the azimuth angle ϕ is defined as the angle between x-axis and the polarization of incident light. For each incident azimuth measurement, our method is similar to that proposed by Bartlett *et al.*[10]. First, the incident polarizer is set to the desired azimuth angle $\phi = 0^\circ - 90^\circ$, the incident light intensity is recorded as I^i_ϕ; the collected light consists of two components, which include a 5%—10% parallel component scattered from the top layer of the sample $I^{\rm s}_{//{\rm upper}}$, and 40% of the light travelling deeper into the sample is multiply scattered and loses its original polarization and re-emitted light passes through the analyzer as 20% of parallel light $I^{\rm s}_{//{\rm bottom}}$. Next, the incident polarizer is rotated and is set to $\phi = 90^\circ$, the collected light contains no light from the top layer and only multiply scattered light from the bottom layer, $I^{\rm s'}_{//{\rm bottom}}$. Subtracting the second intensity measurement from the first gives

$$\Delta I = I^{\rm s}_{//{\rm upper}} + I^{\rm s}_{//{\rm bottom}} - I^{\rm s'}_{//{\rm bottom}} \approx I^{\rm s}_{//{\rm upper}}. \quad (1)$$

Consider an experiment in which the linearly polarized incident light with wavelength λ and azimuth angle ϕ, intensity I_0, is distributed over solid angle $\Delta\Omega_0$, and the scattering light is collected over solid angle $\Delta\Omega$. According to Mie theory, the intensity that is parallel to the polarization of the incident light is then given by

$$I^{\rm c}_{//}(\theta,\varphi,\lambda) = \frac{I_0}{k^2 r^2} \int\limits_{\Delta\Omega} {\rm d}\hat{s} \int\limits_{\Delta\Omega_0} {\rm d}\hat{s}_0 \times [\cos^4\varphi\cos^2\theta\left|S_2^2\right| + \sin^4\varphi\left|S_1^2\right| + 2\cos^2\varphi\sin^2\varphi\cos\theta{\rm Re}(S_1 S_2^*)], \quad (2)$$

where $S_1(\theta)$ and $S_2(\theta)$ are amplitude functions based on Mie theory; θ is the backscattering angle. In our experiment setup, incident light solid angle is sufficiently small and approximately equal to zero, $\Delta\Omega_0 \approx 0$, and it has the possibility to be scattered by many different sized particles. Summing these combined effects, the measured data ΔI is given by

$$I^{\rm c}_{//}(\theta,\varphi,\lambda) = \frac{I_0}{k^2 r^2} \int\limits_{d_1}^{d_2}\int\limits_{\theta_1}^{\theta_2} [\cos^4\varphi\cos^2\theta\left|S_2^2\right| + \sin^4\varphi\left|S_1^2\right| + 2\cos^2\varphi\sin^2\varphi\cos\theta{\rm Re}(S_1 S_2^*)] f(x)\sin\theta{\rm d}\theta{\rm d}x, \quad (3)$$

where d_1 and d_2 are size distribution range; θ_1 and θ_2 are collecting solid angle range; $f(x)$ is the PSD. A Gaussian size distribution was assumed in this study. In each azimuth measurement, when incident polarizer is set to be parallel or perpendicular, respectively, the collected total intensity is

$$I^{\rm c}_{\rm total} = I^{\rm c}_{//{\rm incident}}(\theta,\varphi,\lambda) + I^{\rm c}_{\perp{\rm incident}}(\theta,\varphi,\lambda). \quad (4)$$

In order to eliminate difference of the incident light intensity I_0 in different azimuth angles, according to Eq. (1), the azimuth dependence caused by the hardware can be normalized by

$$\frac{I^{\rm c}_{//}(\theta,\varphi,\lambda)}{I^{\rm c}_{\rm total}} = \frac{I^{\rm s}_{//{\rm upper}} + I^{\rm s}_{//{\rm bottom}}}{I^{\rm c}_{\rm total}} - \frac{I^{\rm s'}_{//{\rm bottom}}}{I^{\rm c}_{\rm total}} = C\int\limits_{d_1}^{d_2}\int\limits_{\theta_1}^{\theta_2} [\cos^4\varphi\cos^2\theta\left|S_2^2\right| + \sin^4\varphi\left|S_1^2\right| + 2\cos^2\varphi\sin^2\varphi\cos\theta{\rm Re}(S_1 S_2^*)] f(x)\sin\theta{\rm d}\theta{\rm d}x, \quad (5)$$

where C is a constant related to the experimental setup and experimental parameters.

The data presented above is obtained by averaging ten frames at each azimuth angle. This serves as ensemble-average of the light scattered by the sample to eliminate the effects of speckle. Furthermore, the perpendicular or parallel polarization intensity is divided by the total intensity to eliminate total intensity difference as the effects of speckle, only the light intensity linearity effects are analyzed.

The feasibility of our experiment method was tested with phantoms. We began by placing suspensions of either polystyrene spheres (Duke Scientific Co.) or HeLa cells atop a strongly scattering substrate consisting of a bulk layer of Intralipid-20% media. The component-azimuth curves of the measured parallel and perpendicular components were collected from a two-layer phantom with the mean diameter of 9 μm and a standard deviation of 0.09 μm polystyrene spheres with a optical thickness of 1 on the top layer. The parallel component of the light is significantly higher than the perpendicular component. Then the parallel component and perpendicular component are subtracted, and then normalized. Figure 2 shows the differential signal and calculated data using Mie theory for the same size distributions and refractive index. The experimental curves are in good agreement with the calculated data. According to the differential signal ΔI, the scatter's size, standard deviation and relative refractive index can be extracted by genetic algorithm inversion according to Eq. (3). The reconstructed size distributions are shown in Fig. 3.

To demonstrate the applicability of the method to biological sample, we conducted experiments with HeLa cells. The mean diameter and standard deviation of cells and nuclei were measured by light microscopy. We obtained the mean diameter of nuclei $d_{\rm n} = 17$ μm, standard deviation $\sigma_{\rm n} = 1.4$, and the mean diameter of cells $d_{\rm c} = 36$ μm, standard deviation $\sigma_{\rm c} = 1.8$. As before,

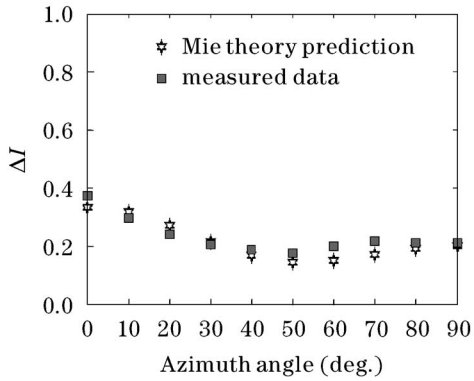

Fig. 2. Comparison of the measured differential signal ΔI of polystyrene spheres to the prediction data based on Mie theory calculation.

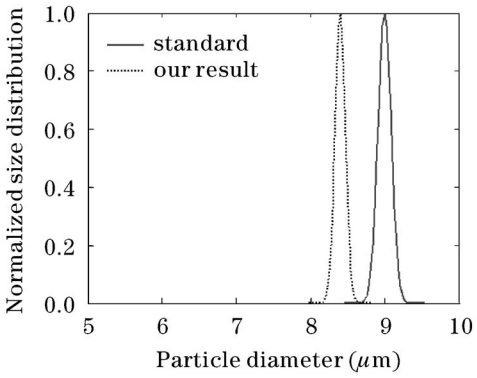

Fig. 3. Comparison of microspheres PSD extracted from ΔI to the standard PSD provided by the manufacturer.

the upper layer consisted of suspensions of HeLa cells, with $\tau \approx 1$. As pointed out in Ref. [3], elastic scattering by cells is due to a variety of cellular organelles, including mitochondria, a variety of endosomes and other cytoplasmic vesicles, and nuclei. The smaller organelles are responsible for large angle scattering, whereas the nucleus contributes to scattering at small angles. So the backscattering intensity is mainly with scattering by nuclei. In Mie theory predictions, the refractive index of nuclei $n_{\rm s} = 1.43$—1.45, the refractive index of the surrounding media $n_{\rm m} = 1.36$—1.38[13]. Figure 4 shows the

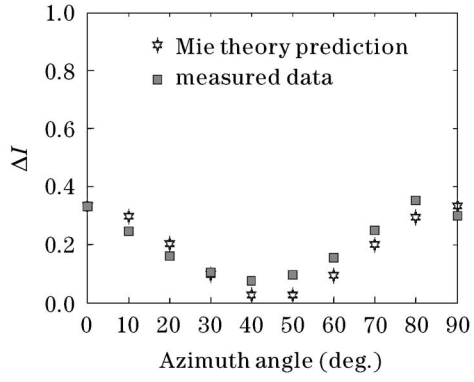

Fig. 4. Comparison of the measured differential signal ΔI of HeLa cells to the prediction data based on Mie theory calculation.

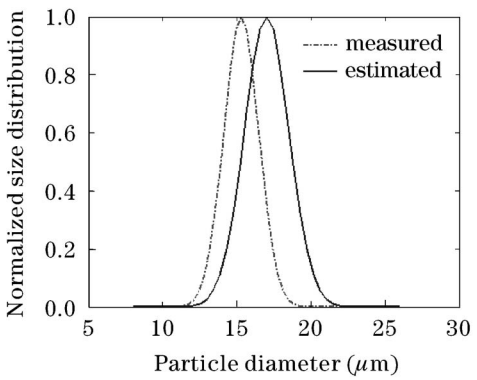

Fig. 5. HeLa cells size distributions extracted from ΔI and estimated from the fluorescence microscope measurement.

measured differential signal dependent on azimuth angle. According to the differential signal, the inversion results are mean diameter $d = 15.7$ μm, standard deviation $\sigma = 1.2$, relative refractive index $n = 1.12$, as shown in Fig. 5. These results are in good agreement with microscopy measurement. Differences could be attributed to the inherent limitation of optics elements, the azimuth angle mechanical error, and inversion algorithm error.

In summary, by varying the azimuth angle of the incident light, we can simultaneously extract information about the nuclei size distribution, standard deviation, relative refractive index by genetic algorithm inversion procedure. The reconstructed size distribution produced from this method is in good agreement with those obtained from other measurement methods. Our ultimate goal is to measure the nuclear cell size distribution of the epithelium *in vivo*.

This work was carried out at the Key Laboratory of Biomedical Photonics of Ministry of Education, Huazhong University of Science and Technology. This research was supported by the National Natural Science Foundation of China (No. 30470460 and 60278017). The author would like to thank M.S. Rui Hu who helped with the experiment and Dr. JuQiang Lin for generously providing the HeLa cells. Q. Luo is the author to whom the correspondence should be addressed, his e-mail address is qluo@mail.hust.edu.cn.

References

1. R. V. Kuranov, V. V. Sapozhnikova, I. V. Turchin, E. V. Zagainova, V. M. Gelikonov, V. A. Kamensky, L. B. Snopova, and N. N. Prodanetz, Opt. Express **10,** 707 (2002).
2. K.-B. Sung, R. Richards-Kortum, M. Follen, A. Malpica, C. Liang, and M. R. Descour, Opt. Express **11,** 3171 (2003).
3. L. T. Perelman, V. Backman, M. Wallace, G. Zonios, R. Manoharan, A. Nusrat, S. Shields, M. Seiler, C. Lima, T. Hamano, I. Itzkan, J. Van Dam, J. M. Crawford, and M. S. Feld, Phys. Rev. Lett. **80,** 627 (1998).
4. M. B. Wallace, L. T. Perelman, V. Backman, J. M. Crawford, M. Fitzmaurice, M. Seiler, K. Badizadegan, S. J. Shields, I. Itzkan, R. Dasari, J. Van Dam, and M. S. Feld, Gastroenterology **119,** 677 (2000).
5. V. Backman, R. Gurjar, K. Badizadegan, I. Itzkan, R. R. Dasari, L. T. Perelman, and M. S. Feld, IEEE J. Sel.

Top. Quantum Electron. **5,** 1019 (1999).

6. V. Backman, M. B. Wallace,L. T. Perelman, J. T. Arendt, R. Gurjar,M. G. Müller, Q. Zhang, G. Zonios, E. Kline, T. McGillican, S. Shapshay, T. Valdez, K. Badizadegan, J. M. Crawford, M. Fitzmaurice, S. Kabani, H. S. Levin, M. Seiler, R. R. Dasari, I. Itzkan, J. Van Dam, and M. S. Feld, Nature **406,** 35 (2000).
7. R. S. Gurjar, V. Backman, L. T. Perelman, I. Georgakoudi, K. Badizadegan, I. Itzkan, R. R. Dasari, and M. S. Feld, Nature Medicine **7,** 1245 (2001).
8. V. Backman, V. Gopal, M. Kalashnikov, K. Badizadegan, R. Gurjar, A. Wax, I. Georgakoudi, M. Mueller, C. W. Boone, R. R. Dasari, and M. S. Feld, IEEE J. Sel. Top. Quantum Electron. **7,** 887 (2001).
9. R. Drezek, M. Guillaud, T. Collier, I. Boiko, A. Malpica, C. Macaulay, M. Follen, and R. Richards-Kortum, J. Biomed. Opt. **8,** 7 (2003).
10. M. Bartlett and H. Jiang, Phys. Rev. E **65,** 031906 (2002).
11. H. Jiang, Opt. Commun. **226,** 279 (2003).
12. A. Amelink, M. P. L. Bard, S. A. Burgers, and H. J. C. M. Sterenborg, Appl. Opt. **42,** 4095 (2003).
13. Y. Deng, R. Hu, Q. Luo, and Q. Lu, Proc. SPIE **5693,** 10 (2005).
14. J. R. Mourant, T. M. Johnson, and J. P. Freyer, Appl. Opt. **40,** 5114 (2001).